Experimental and Theoretical Analyses of GAWBS Phase Noise in Multi-core Fiber for Digital Coherent Transmission

Naoya Takefushi, Masato Yoshida, Keisuke Kasai, Toshihiko Hirooka, and Masataka Nakazawa
Research Institute of Electrical Communication, Tohoku University, 2-1-1 Katahira, Aoba-ku, Sendai, 980-8577, Japan
tnaoya@riec.tohoku.ac.jp

Abstract: We present the phase noise caused by guided acoustic-wave Brillouin scattering (GAWBS) in a 125-µm four-core-fiber. Phase noise induced by higher-order $TR_{n,m}$ modes was found to be dominant rather than that of the $R_{0,m}$ mode. © 2020 The Author(s)

1. Introduction

Recently, the influence of guided acoustic-wave Brillouin scattering (GAWBS) [1], [2] on digital coherent transmission has received a lot of attention [3-9]. GAWBS has two types of resonance modes, i.e., $R_{0,m}$ modes vibrating only in the radial direction and $TR_{n,m}$ modes vibrating in both the radial and torsional directions. The $R_{0,m}$ modes change the refractive index and cause phase noise in the optical signal, while the $TR_{n,m}$ modes change the refractive index along the azimuthal direction and cause not only phase noise but also depolarization due to birefringence. It has been found that phase noise and depolarization caused by GAWBS greatly affect the performance of digital coherent transmission, especially as regards long distance and high multiplicity [6, 8, 9]. In our previous work, we analyzed the GAWBS-induced phase noise and depolarization in various standard fibers including standard single-mode fiber (SSMF), dispersion-shifted fiber (DSF), and ultra-large-area fiber (ULAF), and found that their magnitude depends strongly on the effective core area [8, 9].

With a view to achieving ultrahigh-capacity space division multiplexing, multi-core fiber (MCF) has recently attracted considerable attention as a new transmission medium. In MCF, there are cores both in the center and in off-center locations. The influence of GAWBS phase noise on MCF transmission, especially the difference between the GAWBS characteristics of the center core and the surrounding cores, has not been clarified yet. It is important to note that the center core is affected only by even GAWBS modes such as $R_{0,m}$ and $TR_{2,m}$, and odd modes such as $TR_{1,m}$ and $TR_{3,m}$ have no impact on single-core fiber (SCF) transmissions because of the anti-symmetric refractive index change. On the other hand, the odd modes may have a non-negligible impact in the surrounding off-center cores in MCF.

In this paper, we evaluate the GAWBS phase noise both experimentally and analytically in a four-core fiber (4CF) with a 125 µm cladding. We show that the phase noise caused by $R_{0,m}$ mode are greatly reduced, while the phase noise due to higher-order modes such as $TR_{1,m}$, $TR_{3,m}$, and $TR_{4,m}$ are newly observed, and as a result, the influence of GAWBS in MCF becomes comparable to that in SCF.

2. GAWBS phase noise measurement in four-core fiber

First, we measured the GAWBS phase noise spectrum in an uncoupled 4CF. Each core had a trench-assisted pure-silica core profile whose effective core area A_{eff} was 88-89 µm^2. The average core pitch was 44.2 µm and the cladding diameter was 125 µm, which means that the four cores were shifted by 51% from the center in the radial direction. The fiber was 36 km long. The GAWBS phase noise spectrum was measured using heterodyne detection between the CW light after propagation and a CW local oscillator. For comparison, we also measured the GAWBS noise in a 35

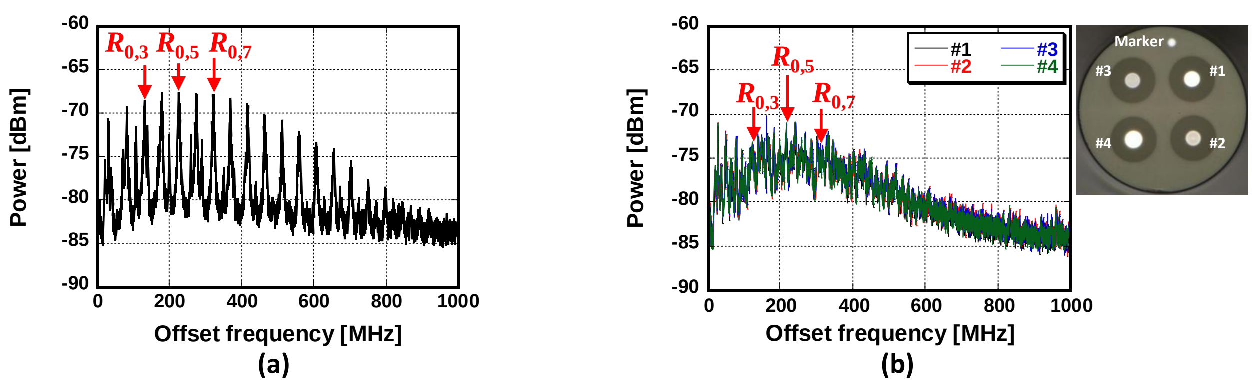

Fig. 1. Heterodyne detected RF power spectra for GAWBS phase noise in 35 km SSMF (a) and 36 km 4CF (b).

km SSMF. Figures 1(a) and (b) show the RF power spectrum of the heterodyne detected signal after propagation over 35 km of SSMF and 36 km of 4CF, respectively. In these figures, the phase noise components of the $R_{0,3}$, $R_{0,5}$ and $R_{0,7}$ modes are highlighted by arrows. In Fig. 1(b), where the phase noise spectra at four cores are superimposed, it can be seen that the four cores exhibit the same phase noise. As the SSMF and 4CF have the same cladding diameter, the resonant frequencies are the same for two fibers. From Fig. 1(a) and (b), it can be found that the power level of the $R_{0,m}$ components are reduced compared with SSMF, but a larger number of small components, which have the appearance of a continuous spectrum, are newly observed in MCF. The ratio of the phase noise magnitude in both fibers, obtained by integrating the phase noise spectrum, was 1 (SSMF): 0.917 (4CF), and therefore the influence of GAWBS in MCF is comparable to that in SSMF.

3. Analysis of GAWBS phase noise in four-core fiber

Next, we analyzed the GAWBS phase noise spectrum in 4CF numerically. The GAWBS phase shift $\delta\phi_{n,m}$ is obtained by employing the overlap integral between the refractive index change $\Delta n_{TRn,m}(r,\theta)$ induced by the $TR_{n,m}$ mode and the optical mode field profile $E(r,\theta)$ [2], which is given by

$$\delta\phi_{n,m} = kl\int_0^{2\pi}\int_0^{a}\{\Delta n_{TRn,m}(r,\theta)\times E(r,\theta)\}rdrd\theta \tag{1}$$

Here, the subscripts n and m represent the order of oscillation in the torsional and radial directions, respectively. Figure 2(a)-(c) show the mode profiles of the optical fields in SSMF and 4CF and the refractive index change caused by the $R_{0,7}$, $TR_{1,7}$, and $TR_{3,7}$ modes. The horizontal axis is normalized by the maximum value. In SSMF, since the mode field is located in the center of a fiber as shown by the black dashed curves, the overlap integral with $\Delta n_{R0,7}(r)$, which is symmetric with a peak at the center, has a large value. On the other hand, the overlap integral between $E(r)$ and $\Delta n_{TR1,7}(r)$ or $\Delta n_{TR3,7}(r)$ becomes zero, as $\Delta n_{TR1,7}(r)$ and $\Delta n_{TR3,7}(r)$ have anti-symmetric profiles. This explains why GAWBS phase noise caused by the $TR_{1,m}$ and $TR_{3,m}$ modes is not observed in SCF.

On the other hand, in 4CF, the mode field is located off-center as shown by the blue curve. This asymmetry causes the overlap integral with $\Delta n_{R0,7}(r)$ to decrease, and this results in the reduction of the phase noise caused by the $R_{0,m}$ modes. Instead, the overlap integral between $E(r)$ and $\Delta n_{TR1,7}(r)$ or $\Delta n_{TR3,7}(r)$ is no longer zero, and the phase shift caused by the $TR_{1,7}$ and $TR_{3,7}$ modes, which was not observed in SCF, becomes dominant in MCF. Moreover, TR modes higher than 4th order also induce a phase shift in MCF. This explains the larger number of phase noise components measured in 4CF as shown in Fig. 1(b).

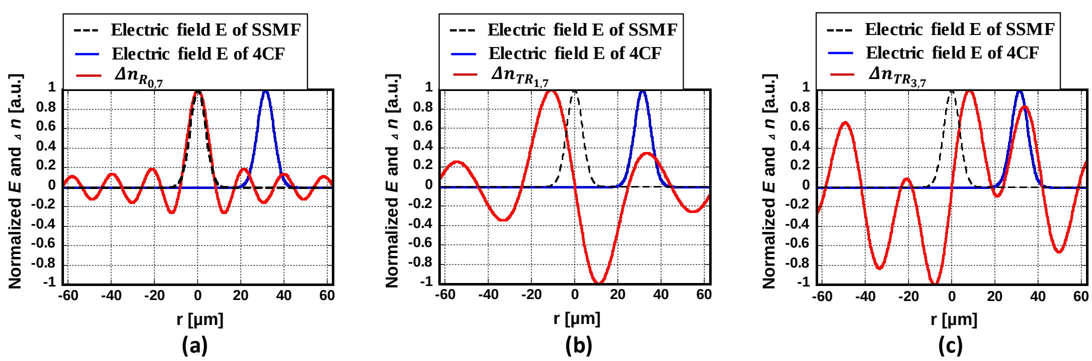

Fig. 2. Overlap between optical electric field $E(r)$ of SSMF (black) and 4CF (blue) and the refractive index change $\Delta n(r)$ caused by the (a) R_{07}, (b) TR_{17}, and (c) TR_{37} modes (red).

We also calculated the modulation frequencies $f_{n,m}$ and the power of the GAWBS phase noise induced by the $R_{0,m}$ ~ $TR_{4,m}$ modes. The resonant frequency $f_{n,m}$ of the acoustic mode is given by

$$f_{n,m} = \frac{V_s}{2\pi a}y_{n,m} \tag{2}$$

where $y_{n,m}$ is the m-th solution of the following equation:

$$\begin{vmatrix} \left(n^2-1-\frac{y^2}{2}\right)J_n(\alpha y) & \left[n(n^2-1)-\frac{y^2}{2}\right]J_n(y)-(n^2-1)yJ_{n+1}(y) \\ (n-1)J_n(\alpha y)-\alpha yJ_{n+1}(\alpha y) & \left[n(n-1)-\frac{y^2}{2}\right]J_n(y)+yJ_{n+1}(y) \end{vmatrix} = 0 \tag{3}$$

Here, a (= 62.5 μm) is the fiber radius, $\alpha = V_s/V_d$ is the ratio of the transverse sonic velocity V_s (= 3740 m/s) to the longitudinal sonic velocity V_d (= 5996 m/s) in quartz glass, and $J_n(y)$ is the n-th order Bessel function. Equation (3) is obtained from the boundary condition where the stress on the cladding surface is zero. The refractive index change $\Delta n_{n,m}(r, \theta)$ induced by the $\mathrm{TR}_{n,m}$ mode is given by

$$\Delta n_{n,m} = \frac{{n_0}^3}{2}\{(P_{11}\cos^2\theta + P_{12}\sin^2\theta)S_{rr} + (P_{12}\cos^2\theta + P_{11}\sin^2\theta)S_{\theta\theta} - (P_{11} - P_{12})\cos\theta\sin\theta\, S_{r\theta}\} \qquad (4)$$

where n_0 is the core refractive index, P_{11} (= 0.121) and P_{12} (= 0.270) are the photo-elastic coefficients of quartz glass, and $S_{rr}(r, \theta)$, $S_{\theta\theta}(r, \theta)$, and $S_{r\theta}(r, \theta)$ are the radial and azimuthal strain profiles in the fiber cross section [10].

The GAWBS phase noise spectrum calculated from Eq. (1)~(4) is shown by the dots in Fig. 3, where the modulation frequency $f_{n,m}$ is shown on the horizontal axis and the optical phase shift $\delta\phi_{n,m}$ is plotted on the vertical axis on a log scale. Here $\Delta n_{\mathrm{TR}n,m}(r,\theta)$ is averaged with respect to θ by integrating from $\theta = 0$ to 2π in Eq. (4) as the polarization state of the optical signal rotates randomly during propagation through a fiber. For comparison, the GAWBS spectrum, whose background noise (- 89.8 dBm) is removed, as an offset from the measured RF spectrum (Fig. 1(b)) is also shown by the black curve. It can be seen that the calculated profile is in good agreement with the experimental data. The experimental results are somewhat lower than the calculated values at lower frequencies. This is due to the leakage of the acoustic wave into the outer polymer jacket in lower modes [11], which is not taken into account in the present theoretical model. The calculated modes between 300 and 600 MHz have weak power levels compared with the measurement. This indicates that $\mathrm{TR}_{n,m}$ modes with $n \geq 5$ play an important role at those frequencies.

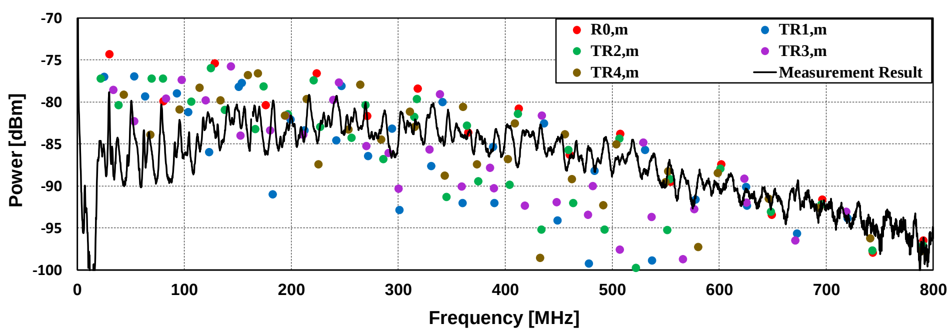

Fig. 3. Comparison of measured GAWBS phase noise spectrum and calculated values for the $\mathrm{R}_{0,m}$ ~ $\mathrm{TR}_{4,m}$ modes.

4. Conclusion

We presented our experimental and theoretical analyses of the GAWBS phase noise generated in 4CF with a 125 μm cladding. Unlike SCF with a core in the center, off-center cores in MCF are dominantly affected by higher-order $\mathrm{TR}_{n,m}$ modes rather than the $\mathrm{R}_{0,m}$ mode. The magnitude of the phase noise in 4CF was comparable (approximately 90%) to that of SSMF.

Acknowledgements

This work was supported by the Ministry of Internal Affairs and Communications (MIC), Research and Development of Innovative Optical Network Technology for a Novel Social Infrastructure (OCEANS). The 4CF was supplied by Sumitomo Electric Industries, Ltd.

References

[1] R. M. Shelby, M. D. Levenson, and P. W. Bayer, "Resolved forward Brillouin scattering in optical fiber," Phys. Rev. Lett. **54,** 939-942 (1985).
[2] R. M. Shelby, M. D. Levenson, and P. W. Bayer, "Guided acoustic-wave Brillouin scattering," Phys. Rev. B **31,** 5244-5252 (1985).
[3] M. Nakazawa, M. Yoshida, M. Terayama, S. Okamoto, K. Kasai, and T. Hirooka, "Observation of guided acoustic-wave Brillouin scattering noise and its compensation in digital coherent optical fiber transmission," Opt. Express **26,** 9465-9181 (2018).
[4] M. Nakazawa, M. Terayama, S. Okamoto, M. Yoshida, K. Kasai, and T. Hirooka, "Observation of guided acoustic-wave Brillouin scattering and its digital compensation in coherent QAM transmission," OFC 2018, M4B.2.
[5] M. A. Bolshtyansky, J. -X. Cai, C. R. Davidson, M. V. Mazurczyk, D. Wang, M. Paskov, O. V. Sinkin, D. G. Foursa, and A. N. Pilipetskii, "Impact of spontaneous guided acoustic-wave Brillouin scattering on long-haul transmission," OFC 2018, M4B.3.
[6] M. Yoshida, N. Takefushi, M. Terayama, K. Kasai, T. Hirooka, and M. Nakazawa, "Reverse phase modulation technique for GAWBS noise error floor elimination in 1024 QAM-160 km digital coherent transmission," OECC 2018, 4B1-3.
[7] M. Paskov, M. A. Bolshtyansky, J. -X. Cai, C. R. Davidson, D. G. Foursa, and A. N. Pilipetskii, "Observation and Compensation of Guided Acoustic-Wave Brillouin Scattering in Modulated Channels," OFC 2019, Tu3J.3.
[8] N. Takefushi, M. Yoshida, K. Kasai, T. Hirooka, and M. Nakazawa, "GAWBS noise characteristics in digital coherent transmission in various optical fibers," OECC 2019, ThC2-5.
[9] N. Takefushi, M. Yoshida, T. Hirooka, K. Kasai, and M. Nakazawa, "Experimental and theoretical analyses of GAWBS depolarization noise in digital coherent transmissions," ECOC 2019, Tu.1.C.1.
[10] E. K. Sittig and G. A. Coquin, "Visualization of plane-strain vibration modes of a long cylinder capable of producing sound radiation," J. Acoust. Soc. Am. **48,** 1150-1159 (1970).
[11] A. J. Poustie, "Bandwidth and mode intensities of guided acoustic-wave Brillouin scattering in optical fibers," J. Opt. Soc. Am. B, **10,** 691-696 (1993).